An Integrated Health Management System Approach: Application to Shipboard Rotating Machinery

Edward W. Mayfield[1], Guangxing Niu[2], Bin Zhang[3], Paul Ziehl[4], and Michael Golda[5]

[1,2,3] *Department of Electrical Engineering, University of South Carolina, Columbia SC 29208*

mayfiele@email.sc.edu
gniu@email.sc.edu
zhangbin@cec.sc.edu

[4] *Department of Environmental and Civil Engineering, University of South Carolina, Columbia SC 29208*

ziehl@cec.sc.edu

[5] *Naval Surface Warfare Center, Philadelphia Division (NSWCPD), Philadelphia, PA*

eugene.m.golda1@navy.mil

ABSTRACT

This paper aims to develop an integrated shipboard condition prognostics system that integrates sensing, data processing, feature extraction, and fault diagnostic and prognostic algorithms with applications to rotating machinery. The proposed system is designed and implemented with an application case of a number of bearing systems of seeded faults at different fault dimensions. The overall system design, experimental design and platform, bearing fault modes analysis, feature extraction, fault dynamics modeling, diagnostics and prognostics design, and human-machine interface are discussed with details. The proposed effort aims to provide effective assessment of the condition of shipboard rotating machinery systems and lower the overall operation and maintenance (O&M) cost. The proposed work is tested on data of bearings with various fault modes, models with multiple interactive faults, and experimental testbed as a whole system. The proposed condition prognostics system is scalable, generic, easy-to-implement, and mathematically rigorous, which can be applied to a variety of Navy applications.

1. INTRODUCTION

Navy shipboard machinery systems are crucial components to accomplish critical military missions safely and reliably. Traditional maintenance practices rely on breakdown or schedules that are not only labor intensive, but also lead to unexpected downtime and increased operation and maintenance (O&M) cost (Leger and Iung, 2012). More recently, condition-based maintenance (CBM) adopts a paradigm shift for maintenance of complex machines and large-scale assets. Fault diagnosis and prognosis (FDP) and nondestructive evaluation/structural health monitoring (NDE/SHM) are fundamental enabling technologies for CBM. However, traditional approaches are facing challenges with requirements in terms of scalability and real-time implementation.

First, traditional FDP algorithms focus on a single component. Although multiple faults from multiple components are considered in some existing approaches, they treat each fault individually as an isolated case. In real applications, a fault or degradation on a component or subsystem is often interacting with or has influence on faults (or degradations) on other components or subsystems, resulting in cascading failure. These interacting faults form a multidimensional FDP problem that challenges the traditional approaches, both in theory and implementation.

Second, most techniques found in literature only use diagnostic information to react to faults (Zhang et. al, 2011; Yu et. al, 2013; Flett and Bone, 2016; Zhou et. al, 2016, Zhao et. al, 2017). These techniques cannot overcome the fact that they are reactive paradigms. That is, these techniques are only activated by the detection of faults and maintenance is only optimized based on current health condition without consideration of prognostic information, which predicts the fault state in a future time instant and estimates the remaining useful life (RUL) (Orchard et. al, 2013; K. Singleton et. al, 2015). As a result, these strategies may not be optimal over a long period of time. By

integrating RUL in maintenance, it improves the reactive CBM strategies to prognostics-enhanced proactive strategies, making systems more reliable, operationally available, and economically maintained. In addition, the utilization of information about fault state and RUL enables the evaluation of the effects of faults on system performance and risk of mission failure. This can be used to avoid undesirable states and operating modes to defer potential failure through optimal use strategies and planning.

Third, real-time FDP is always a challenge especially when distributed FDP is widely accepted in which FDP functions are deployed on local microprocessors and embedded systems. The distributed FDP has advantages of low-cost and high reliability. However, due to their low capabilities in computation, storage, and communication, these local processors cannot afford traditional FDP algorithms with high computational complexity. Only very simple FDP functions, such as limit checking, trend analysis, etc. can be applied, which sacrifice performance in terms of accuracy, precision, and robustness. To address this problem, we propose a particle filtering based FDP algorithm for distributed real-time implementation.

To overcome these challenges, under the sponsor of Navy Engineering Education Consortium (NEEC), this paper proposes a low-cost distributed shipboard condition prognostics system (SCPS) that is enabled by sensing, data acquisition and analysis, feature extraction, fault dynamic modeling, particle filtering-based diagnosis and prognosis, operation risk evaluation, and decision-making to reduce O&M cost and assure critical Navy mission accomplishment, as shown in Fig. 1. The research goals are to accommodate the growing demands of distributed Navy shipboard machinery systems in aspects of economy, optimality, reliability, and safety. The proposed condition prognostics system is scalable, generic, easy-to-implement, and mathematically rigorous, which can be applied to a variety of Navy applications. The proposed solution is verified with laboratory possessed data, models, and a rotating machine test bed. Since it is the first year of the project, the focus of this paper is mainly on data acquisition, processing, feature extraction and fault diagnosis and prognosis.

The paper is organized as follows: Section 2 discusses the bearing system and bearing testbed; Section 3 provides the diagnosis and prognosis structure; Section 4 develops a case study of bearing fault diagnosis and prognosis, which is followed by concluding remarks given in Section 5.

2. THE BEARING DATA AND TESTBED

Since bearings are widely used in machinery, bearing failures are common causes for system breakdowns, which typically result in a catastrophic event or costly downtime if such failures are not detected correctly in time. Factors that determine the useful life of bearings include material properties, lubricant properties, bearing size, number of rolling elements, load/speed of bearing, installation, etc. (Howard, 1994; Grill, 2017, Zhang et al. 2008). Health monitoring or condition-based maintenance of bearing includes anomaly detection, fault diagnosis, and failure

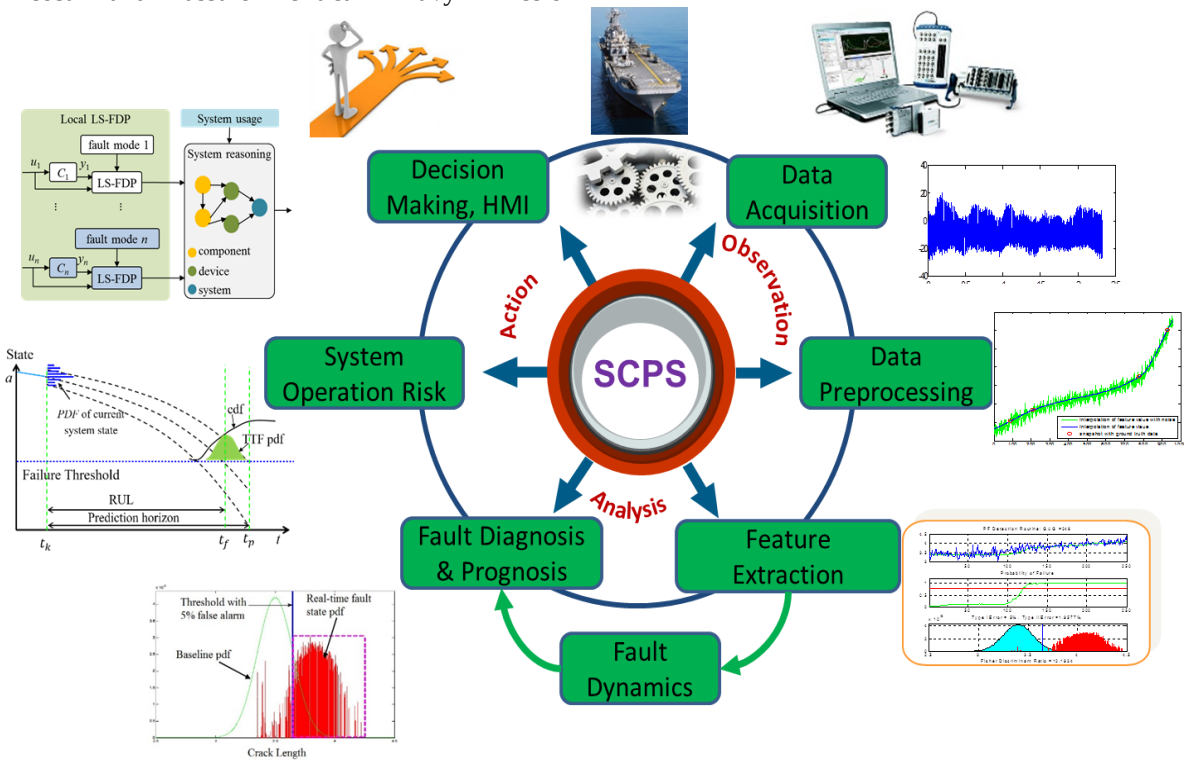

Figure 1 The scheme of the proposed SCPS

prognosis. Anomaly detection is used to determine the occurrence and existence of a fault in the machine bearing whereas diagnosis localizes the fault and determines the type of fault. Finally, failure prognosis estimates the remaining useful life (RUL) of the damaged bearing.

2.1. Bearing Testbed

A rolling element bearing usually consists of an inner ring, outer ring, a number of rolling elements (balls or rollers), and a cage. The inner and outer rings have raceways that form a path, which allows the rolling elements rotating along to provide minimal friction for rotational movement. The rolling elements are designed to allow them contacting the raceways at a single point. The cage maintains an even and consistent spacing of rolling elements in the raceways during movement.

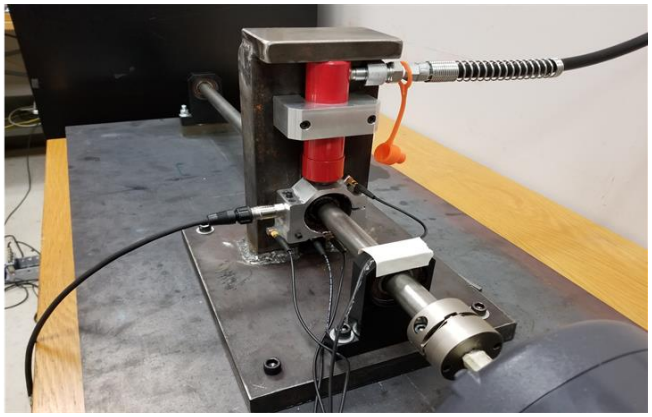

Figure 2. The rotating machine test bed

A rotating machine test bed is necessary in order to simulate shipboard bearing conditions and collect vibration data for algorithm development. This machine in Fig. 2 is designed to provide maximum control over the test bearings load and speed while allowing easy access for instrumentation and bearing replacement. The tested bearings have an inner diameter 25mm, outer diameter of 52mm, and are rated for a maximum radial load of 3200 pounds. To simulate an overload scenario at different speeds, the machine is capable of applying variable load of up to 4000 pounds and variable speed up to 1200 rpm. During experiments, acoustic emission sensors and accelerometers collect data from the bearing housing that is processed and used to test the diagnosis and prognosis algorithm.

The test bed includes several major components including a 3-phase motor, variable frequency drive (VFD), and hydraulic system. To simulate the bearing environment, the test bed uses a 3-phase 2 horsepower motor to rotate the shaft at speeds up to 1200rpm while testing various loads up to and beyond the bearings rated capacity. A hydraulic system is used to apply load rather than a weight-based system for safety and ease of use. To power the motor, a VFD is used that can be programed to automatically cycle through speeds and can be controlled by external signals sent from the computer running the prognosis algorithm. An acrylic shield is also used for safety when the machine is running to protect the operator in the event of mechanical failure.

2.2. Test Plan

The primary wear conditions in the experiments are overload, lack of lubrication, and introduction of abrasive materials to the bearing. Although rotational speed is a contributing factor to the rate of bearing wear, over-speed is not currently being tested as a primary source of failure since the bearings are rated up to 10000rpm. Speed is varied while testing the wear conditions to ensure the accuracy of the prognosis algorithm in a dynamic system and across a range of speeds.

Bearings are subjected to 8-hour tests at 600lb load to establish a baseline of bearing noise characteristics and then are tested at 2800, 3200 and 3600 pounds for 8 hour each. During tests, rotational speed is cycled through 1-minute periods of 600, 900, and 1200rpm (Fig. 3) to simulate a variable speed system and sample vibration data at different speeds. The same test is performed for various lubrication scenarios including under-lubrication, no lubrication, and incorrect lubricant. Future tests are adapted based on these results. If needed, tests can be repeated until a bearing shows signs of degradation. The progression of the bearing condition from healthy to failure is record and used to develop the diagnosis and prognosis algorithm. After the test is completed and the bearing is sufficiently degraded, it is disassembled and inspected for inner race, outer race, and rolling element faults. Comparison between recorded data, algorithms prognosis, and physical inspection are being made to improve the algorithms effectiveness.

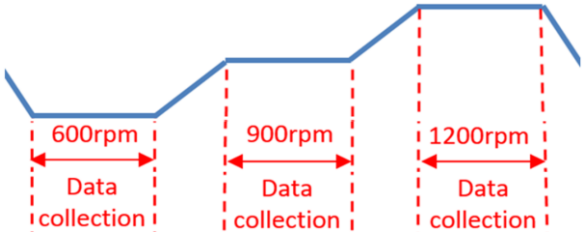

Figure 3. Speed cycling during experiments

2.3. Bearing Fault Modes

When bearings are under load, the bearing operation related parameters are shown in Fig. 4, where P is the load, $\emptyset$ is the extent of load zone, φ is the angle of load on the rolling element, and P_{max} is the maximum radial load.

The rotating component could be either the inner ring or the outer ring. For a bearing in most motors, the outer ring can be assumed stationary since it is generally locked on the stator. Therefore, we focus on this operating condition. The

loading type could be either radial or axial. In the case of axial loading, the load on any rolling element at any arbitrary position is constant as shown in Figure 4(a). Therefore,

$$P(\omega_s t) = P \tag{1}$$

with ω_s being the rotating frequency of shaft.

For radial loading, the load of a certain rolling element changes with its angular position, as shown in Figure (b). The load on the rolling element at an angle φ can be written as:

$$P(\varphi) = \begin{cases} P_{max}[1 - 0.5\varepsilon(1 - \cos\varphi)]^q & -\emptyset \le \varphi \le \emptyset \\ 0 & otherwise \end{cases} \tag{2}$$

where $q = 10/9$ for roller bearings. The load zone $\emptyset$ and the maximum load P_{max} are given by:

$$\emptyset = \cos^{-1}(1 - 2\varepsilon);\ P_{max} = 5P/Z\cos\alpha \tag{3}$$

where $\varepsilon, Z,$ and α are the load distributor, number of rolling elements, and contact angle, respectively.

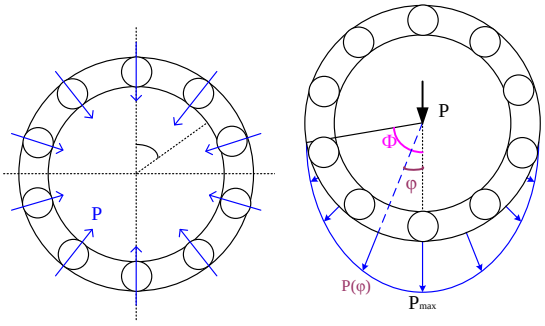

(a) Axial loading (b) Radial loading

Figure 4. Different loading types

The rotating speed is often given by rpm and denoted as f_m, from which, the angular velocity of the shaft in unit rad/second (ω_s) can be calculated as $\omega_s = f_m/(60 \times 2\pi)$.

The angular velocity of the cage (ω_c), or the fundamental train velocity is:

$$\omega_c = \frac{\omega_s}{2}\left(1 - \frac{d}{d_m}\cos\alpha\right) \tag{4}$$

The frequency of rotation of the rolling elements about their own axes, i.e., ball spinning frequency (ω_b), is given by the cage rotating frequency multiplied by the ratio of the inner race to the ball diameter.

$$\omega_b = \frac{\omega_s d_m}{2d}\left(1 - \left(\frac{d}{d_m}\cos\alpha\right)^2\right) \tag{5}$$

When a fault occurs, assuming no slip, every time the rolling elements contact the defect, an impulse force is generated at the fault characteristic frequency. For a defect on the inner raceway, outer raceway, and rolling elements, the fault characteristic frequencies are given by $\omega_{id}, \omega_{od}, and\ \omega_{bd}$, respectively and are calculated as follows (Onel et. al, 2005):

$$\omega_{id} = \frac{Z\omega_s}{2}\left(1 + \frac{d}{d_m}\cos\alpha\right) \tag{6}$$

$$\omega_{od} = \frac{Z\omega_s}{2}\left(1 - \frac{d}{d_m}\cos\alpha\right) \tag{7}$$

$$\omega_{bd} = \frac{\omega_s d_m}{d}\left(1 - \left(\frac{d}{d_m}\cos\alpha\right)^2\right) \tag{8}$$

Apart from this main defect characteristics frequency, sidebands around these frequencies also appear in the spectra. The sidebands of different fault characteristic frequencies are shown in the Table below:

Table 1 Fault characteristic frequencies and sidebands

Fault	Inner race	Outer race	Rolling element
Main	ω_{id}	ω_{od}	ω_{bd}
Sideband	ω_s, ω_c	$\omega_s, \omega_s - \omega_c$	$\omega_c, \omega_s - \omega_c, \omega_b$

2.4. Bearing Vibration Data

Rolling element bearings are the most essential parts in shipboard rotating machinery. For navy mission operations, the bearings are often subject to high loading, corrosive environment, and severe conditions. Under such severe condition, defects can easily occur and degrade the performance of the system or even damage the system if such defects are not detected and actions are not taken. It is therefore of prime importance to accurately detect and estimate the severity the defects, especially at the early stages to prevent sequent damage and reduce the costly downtime. Vibration signal is the mostly commonly used signals for bearing defects detection and identification because the vibration signals from accelerometers providing a wide dynamic range and wide frequency range (Howard, 1994; El-Thalji and Jantunen, 2015).

For a healthy bearing without a fault, the vibration signal shows a regular signature. When a defect occurs, the interaction between the raceway and rolling elements with defects generates time-varying discontinuous forces that change the regular signature. However, this change of regular signature is not obvious in its early stage and need advanced signal processing and detection algorithms.

In general, the bearing defects are classified into local defects and distributed defects (Meyer et. al, 1980; C. M. N. Leite et. al). The former one includes pits, spalls, cracks, while the later one includes misalignment, surface roughness, eccentric raceway, etc. When the bearing operates with distributed defects, it generates a specific vibration signature, increases friction, and eventually leads to local defects.

Vibration data was acquired from a bearing with a naturally occurring spall at a sampling frequency of 204,800 Hz and is measured at different bearing service times. Each segment contains data of 8 second periods. Since bearing lifespans can last for millions of revolutions, there should not be a significant change in condition within a short time. To reduce unnecessary computation and data storage, data can be recorded for short periods of 8 seconds once per minute or every few minutes. During the bearings lifespan, the bearing is disassembled after a certain number of services hours to investigate the health condition of the bearing. The data and health conditions are listed in Table 2.

Table 2 Vibration data and fault dimension

Service time	Data length	Spall area (mm^2)
0		0
1.5 hours	8 seconds	
3.5 hours	8 seconds	
8 hours		0.3×0.2
12 hours		0.4×0.2
13 hours	8 seconds	
15.5 hours	8 seconds	
16 hours		05×0.2

2.5. Bearing Fault Feature Extraction

As the vibration signal does not indicate fault directly, features need to be extracted from vibration signals as an indicator to reveal the characteristics of bearing fault.

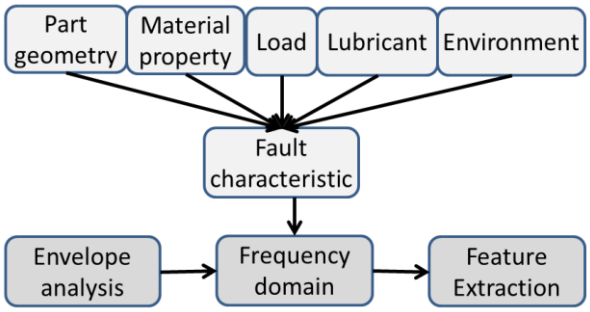

Figure 5. Bearing fault contributing factors and feature extraction

The fault feature extraction can be illustrated in Fig. 5. It is understood that part geometry, material property, loading profile, lubricant condition, and environmental factors are all contributing factors of bearing fault. From the bearing geometry, the fault characteristic frequency can be identified. Then envelope analysis can be conducted and, by investing the spectra of envelope signal in the frequency domain, feature can be extracted for fault diagnosis. More details are provided as follows.

Envelope analysis (Howard, 1994), as one of the most prominent vibration signal processing techniques, has shown success in diagnosis of rolling element bearing faults because it is able to separate the vibration generated by a defective bearing from the vibration generated by other machine components.

When a defect occurs in the bearing, the contact between rolling elements and raceway at the defect area generates an impulse force in the operation. This impulse has a very short time duration compared to the interval between impulses. This short impulse causes energy to spread over a wide range of frequencies in the spectrum. The periodic impulse also leads to repetitive excitation of resonance. The frequency of the impulse is also called the characteristic bearing defect frequency, which is related to the location of fault, bearing rotating speed, and geometric dimension of bearing. By demodulating the vibration signals at the resonance, envelope analysis can detect and locate a fault.

The procedure of envelope analysis is as follows. First, the vibration signal is processed through a band-pass filter. The cutoff frequencies of the band-pass filter are selected such that the filtered signal reverse the component around the resonant frequencies excited by the impulse and, at the same time, remove all other components. Second, the analytical signal of the band-pass filtered signal is built by adding an imaginary part given by the Hilbert transform of the band-pass filtered signal. The absolute value of the analytic signal gives the envelope of the vibration signal, as shown in Fig. 6. Then, the spectrum of the envelope signal shows the components of the fault characteristic frequency via Fourier transform and facilitates the process of feature extraction.

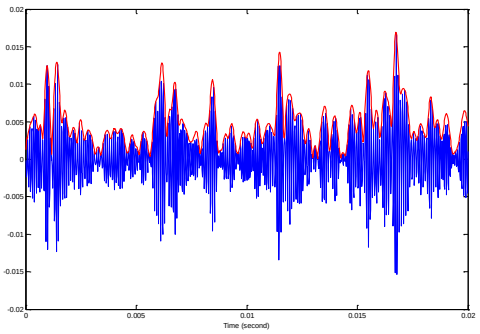

Figure 6. An example of envelope analysis (blue is the original vibration signal and red is the envelope signal).

After the spectrum of the envelope signal is obtained, the energy ratio of components at the fault characteristic frequencies to components at other frequencies are calculated. For robustness, the sum of the first three harmonics is taken. The procedure is described as follows:

First, identify the fault characteristic frequencies up to three harmonics for each fault mode (inner raceway fault, outer raceway fault, and rolling element fault). Since the fault location is not yet determined, all potential frequencies are calculated. Then, identify the sidebands associated with these fault characteristic frequencies and its harmonic

frequency. The energy in these frequencies are summed for inner raceway fault, outer raceway fault and rolling element faults, respectively. The accumulation of energy can be denoted as $E_{ird}, E_{ord},$ and E_{red} for fault characteristic frequencies, harmonics, and sidebands of inner raceway fault, outer raceway fault, and rolling element fault, respectively. Note that as the fault becomes more severe, the energy on these frequency components increases.

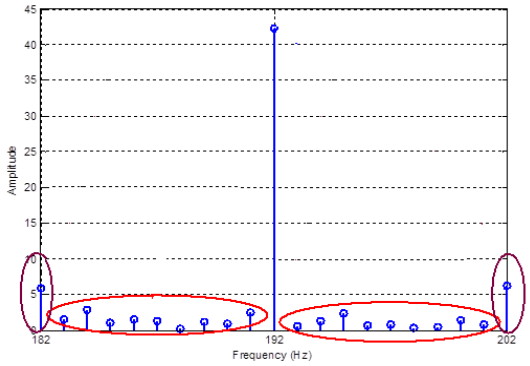

Figure 7. Spectra of envelope signal and identification of fault characteristic frequency (middle blue components), sidebands (two components circled by brown ovals) and background components (other components circled by red ovals)

Second, the energy for all other frequency components (background vibration components), from the sideband with the lowest frequency to the sideband with the highest frequency, are summed, denoted as $E_{irb}, E_{orb},$ and E_{reb} for frequencies on background vibration components around the fault characteristic frequencies of inner raceway fault, outer raceway fault, and rolling element fault, respectively. Note that, since these frequency components are not related to fault impulse, they should theoretically remain unchanged when the fault becomes more severe.

Third, the ratio of $E_{ird}/E_{irb}, E_{ord}/E_{orb},$ and E_{red}/E_{reb} are then used as conditional indicator for inner race fault, outer raceway fault, and rolling element fault. These frequency components are shown in Fig. 7.

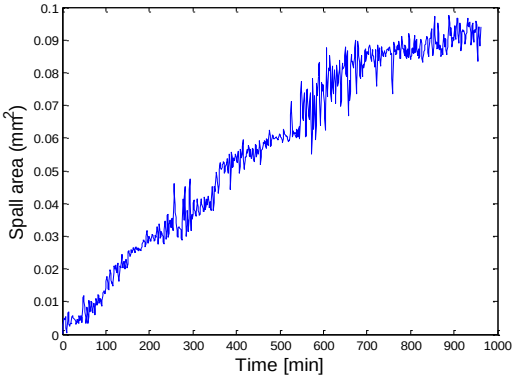

Figure 8. Nonlinear mapping of fault dimension as a function of time obtained from interpolation.

Since only limited data at different service time are available, the data are interpolated for diagnosis and prognosis purpose. Fig. 8 shows the interpolated fault growth curve as a function of time. Note that noises are added to reflect the real system situation. The data in this interpolated curve is used for verification of the proposed algorithm.

3. DIAGNOSIS STRUCTURE

When the bearing is in operation, effective online bearing fault diagnosis and prognosis are challenging, mainly because of the complexity of shipboard environment. After feature or fault indicator is extracted, advanced algorithm for statistical analysis and estimation is needed. To solve this problem, many fault detection algorithms were developed with successes. In this research, Bayesian estimation method is employed as it integrates the modeling of fault dynamics and measurement to achieve estimation of fault state. Fig. 9 shows the chart with information flow.

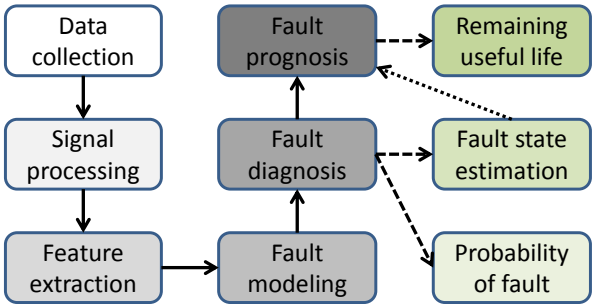

Figure 9. Diagnosis and prognosis with information flow

3.1. Fault dynamic modeling

In this paper, a particle filtering algorithm is used for fault state online monitoring and estimation. For particle filtering based method, a fault degradation model is needed to describe the fault dynamics.

The fault growth in the bearing can be modeled by cyclic loads acting on the rolling surface. Paris law (Paris, 1963) is often used for this purpose, which is given as:

$$\frac{da}{dR} = C(\Delta K)^n \qquad (9)$$

This model describes the fault dimension growth increment *da* per cycle *dR*, *a* is the fault dimension, *R* is the number of rotating cycles, *C* and *n* are material constants, and ΔK is the stress intensity factor.

Note that a relationship representing the stress intensity factor as a function of the loading profile and fault dimension can be difficult to get. To develop a simple, model, Eq. (1) is modified as

$$\frac{dD}{dt} = C(D)^n \quad (10)$$

that is the rate of fault growth under the instantaneous fault dimension *D*, which is the area of spalling, under a steady operating condition in a given time interval.

Based on this equation, a fault growth model in the discrete-time form can be written as:

$$D(k+1) = D(k) + C(D(k))^n \quad (11)$$

Since fault dimension cannot be measured directly, it is assumed that the extracted feature and fault dimension has a one-to-one mapping. Therefore, the extracted feature can be used for diagnosis purpose.

The performance of this model and the overall approach presented here were assessed using data from different bearings and with model parameters adaptation (Zhang et. al, 2010).

3.2. Particle filtering for diagnosis and prognosis

In the past decades, many diagnosis and prognosis algorithms were developed (Berecibar et. al, 2016). Bayes theory based algorithms, including Kalman filter, Extended Kalman filter, particle filter are very suitable for the problem of real-time state estimation (Bangjun et. al, 2017; Orchard and Vachtsevanos, 2007) . The advantages of these methods are that they incorporate process data into an a priori state estimate by considering the likelihood of sequential observations. Moreover, the noise term in the model can be adjusted to reflect the confidence on the mode. If a well-designed model is developed, the noise can be selected as a very small value. On the other hand, if a rough model is used, the noise needs to be set to a sufficiently large value. The trade-off is that the estimated results tend to be noisy when large noises are used.

In this work, particle filtering is used due to its capabilities in dealing with nonlinear and non-Gaussian systems. In particle filter, real-time diagnosis aims to estimate recursively the current fault state by taking into account available measurements. It involves two steps: prediction and filtering. Prediction is to estimate the priori probability density function (PDF) of the state by using the process model:

$$x_k = f_k(x_{k-1}, u_{k-1}, \omega_{k-1}) \quad (12)$$

where x_k, u_k, and ω_k are the state, input, and noise at time k, respectively, f_k is a nonlinear function as the one shown in Eq. (11) for bearing. Note that the input can be any factors that affect the fault growth such as loading profile and environmental factors. Here, f_k is used to make the description concise and generic.

The filtering step updates the priori PDF generated from prediction with the measurement to get the posterior PDF through the use of the measurement model:

$$y_k = h_k(x_k, v_k) \quad (13)$$

where y_k is the measurement given by the features extracted from the raw data, h_k is a nonlinear function that denotes the nonlinear mapping from fault state to feature, and v_k is measurement noise. As mentioned early, if such a mapping is not available, feature values can be used as fault state for diagnosis directly. In that case, Eq. (13) reduces to $y_k = x_k + v_k$. This does not affect the implementation of diagnosis.

In particle filter, the distribution is represented by a set of particles. Each particle is a sample in the state space with a weighting factor $\left\{x_{0:k}^{(i)}, w_k^{(i)}\right\}_{i=1,\cdots,N}$, $w_k^{(i)} > 0$ and $\sum w_k^{(i)} = 1$. This set of N particle can be used to approximate the behavior of a desired probability distribution, i.e. the fault state distribution, $\{\pi_k\}$. For the posteriori fault state PDF given by $\left\{x_{0:k-1}^{(i)}, w_{k-1}^{(i)}\right\}$ at time instant $k-1$, diagnosis aims to generate a new set of particles $\left\{x_{0:k}^{(i)}, w_k^{(i)}\right\}$ from process model and measurement such that the fault state PDF at time instant t can be accurately approximated.

According to particle filter, the posterior PDF can be approximated by

$$p(x_k|y_{1:k}) \approx \sum_{i=1}^{N} w_k^{(i)} \delta\left(x_k - x_k^{(i)}\right) \quad (14)$$

where $w_k^{(i)}$ is the weight of the i-th particle at time k and $\delta(\cdot)$ is the Dirac delta function. The weights are updated as:

$$w_k^{(i)} = w_{k-1}^{(i)} p\left(y_k|x_k^{(i)}\right) \quad (15)$$

From above equations, the fault state PDF, $p(x_k|y_{1:k})$ at time k can be calculated. This PDF is then compared with a baseline state distribution, which is constructed from the data when the bearing is in normal operating condition and has no fault, to claim whether a fault is detected. The statistical confidence of fault detection can be given by the sum of the weights of the particles whose states are larger than a threshold, which is defined by false alarm rate.

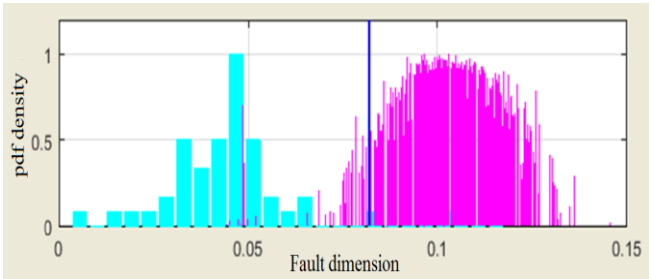

Figure 10. Particle-filter-based diagnosis. The cyan histogram represents the baseline data, while the magenta distribution is the particle-filter-based PDF estimate for the current bearing fault. The vertical line represents the threshold for a 5% false alarm rate.

Fig. 10 shows the results from the proposed approach being applied to bearing fault detection with fault model (x) and 500 particles. The cyan histogram is the baseline distribution from the bearing with health condition while the magenta distribution is the real-time estimation of fault state. The blue vertical line is determined by the 5% false alarm rate, which is predefined. It must be noted that, in this approach, no particular specification about the detection threshold has to be made prior to the actual experiment. Customer specifications, such as false alarm rate, are translated into acceptable margins for false positives and false negatives in the detection routine. The algorithm itself indicates when the false positives and false negatives have decreased to the desired level.

When fault state is estimated, prognosis is triggered to project the current fault state PDF into future time instants. Then these fault state distributions are compared with a failure threshold to predict the time to failure or remaining useful life. Note that when the current fault state is projected into the future time instant, no measurement is available. Therefore, only the priori distribution is calculated using the model given by Eq. (12). That is, only the prediction step is conducted while no filtering step. Because of this, the uncertainty associated with the prior PDF will increase as the prediction horizon increase. This is one of the major challenges in prognosis.

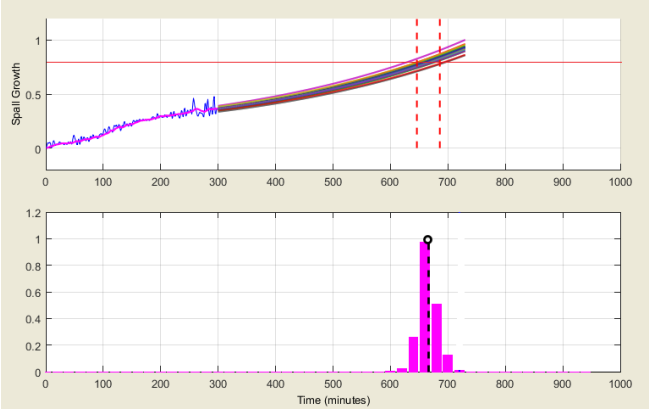

Figure 11. Particle-filter-based prognosis. In the upper subfigure, the prediction curve of each particle is shown with different colors, the red horizon line is the failure threshold, and the vertical dotted lines show the 95% confidence interval. In the lower subfigure, the magenta histogram shows the time to failure distribution and the dotted line shows the mean value of this distribution.

Moreover, since the prognosis calculation involves recursive implementation of prediction of each particle, this is a very time consuming process especially when the prediction horizon is large. This is the second major challenge of prognosis. To address this problem, the number of particles is reduced to 20 to make real-time implementation possible at the cost of reduced accuracy. Fig. 11 shows an example of prognosis started from the 300th minutes, which shows the prediction of each particles (given by the prediction curves with different colors) and RUL distribution (given by magenta histogram).

4. GRAPHIC USER INTERFACE

The paper aims to introduce a SCPS, which integrates data acquisition, data pre-processing, feature extraction, fault dynamics modeling, FDP, system operating risk evaluation, and decision-making. To demonstrate the approach described, it is applied to bearing data and integrated into a graphical user interface (GUI). The GUI displays the results of the integrated algorithms for data processing, feature extraction and diagnosing. The GUI shows real-time system health information and allows operators to understanding the system health condition. It is of interest to incorporate information about fault state PDF estimation so that it provides not only a deterministic decision but also probabilistic and statistical result for decision-making.

Fig. 12 shows the design GUI, in which area A is for component selection as it is assumed that the program can be used for multiple components, Area B is the original vibration data and the feature extracted, Area C shows some performance related information, Area D shows the graphic results of diagnosis and prognosis, and Area E shows some diagnosis results alarms by using different color codes.

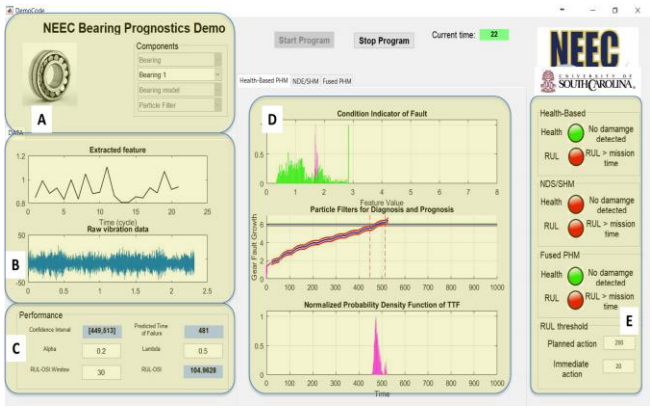

Figure 12. Graphic user interface

The interaction of the GUI with the fault dynamic model is conducted through a middle agent, which is in charge of ensuring that all communication with the model block is performed appropriately. This middle agent conducts the following tasks: pass all parameters and variable to the model block; execute the model as needed; provide initial condition on initial fault state and parameters; and error handling. Therefore, the middle agent is a link between the simulation or real-time program and the model.

When an external application or function, which can be either a simulation or a real-time program, makes a call to the model, the model runs with the parameters and initial

condition from middle agent. The outcome from the model, which is the fault detection probability and fault state estimation are returned to middle agent, which can be further sent to GUI for display. This structure is shown in Fig. 13, which shows that middle agent is a connection between GUI and model for diagnosis, while the GUI can be used for offline simulation or online real-time monitoring.
The experimental setup has been connected with the GUI to monitoring bearings under test. Experimental results on available dataset have been tested and verification. With the bearing under test on the experimental testbed described in Section 2, the research is putting efforts on onboard system monitoring and real-time data processing, diagnosis, and prognosis. The other functional units, such as uncertainty management, risk evaluation, multiple fault modes, probabilistic reasoning, and decision-making are being added as the project progresses.

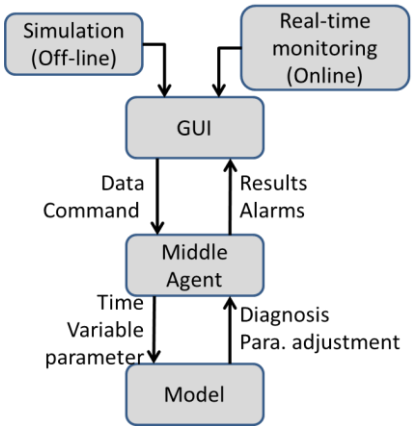

Figure 13. The communication of GUI and model

5. CONCLUSION

This paper introduces the design of an integrated health management approach for shipboard condition prognostics system. The case study with application to bearing system fault diagnosis and failure prognosis are presented. The approach combines a variety of tasks, including data acquisition, data analysis, feature extraction, fault dynamic modeling and particle filtering based algorithm design to enable and enhance the effectiveness of the system health assessments. Bearing dataset is used to verify the effectiveness of the proposed method and it is integrated with a graphic user interface for further development. Preliminary results show that the proposed system has satisfactory performance in diagnosis and prognosis and has advantages such as custom specification to determine fault detection threshold, real-time implementation, and statistical results for probabilistic analysis. The integrated algorithm can accurately detect faults, predict the remaining useful life, and is of a generic design which can be extended to other systems.

ACKNOWLEDGMENT

The research work is supported by Navy Engineering Education Consortium program, Philadelphia division under contract No. N00174-17-1-0006 and the ASPIRE grant program at the University of South Carolina.

REFERENCES

Berecibar M., Gandiaga I., Villarreal I., Omar N., Van Mierlo J., Van den Bossche P. Critical review of state of health estimation methods of Li-ion batteries for real applications. Renewable and Sustainable Energy Reviews. 2016 Apr 1;56:572-87.

El-Thalji I., Jantunen E. A summary of fault modelling and predictive health monitoring of rolling element bearings. Mechanical Systems and Signal Processing. 2015 Aug 1;60:252-72.

Flett J., Bone G.M. Fault detection and diagnosis of diesel engine valve trains. Mechanical Systems and Signal Processing. 2016 May 1;72:316-27.

Gill A. A Research on Fault Detection and Diagnosis of Rolling Bearing. International Journal of Advance Research, Ideas and Innovations in Technology. 2017;3(4):796-807.

Howard I. (1994) A Review of rolling element bearing vibration ”detection, diagnosis and prognosis, DSTO-RR-0013, Airframes and Engines Division

Leger J., Iung B. (2012) Ships fleet-wide management and naval mission prognostics: Lessons learned and new issues, Proc. of IEEE Prognostics and Health Management (PHM), Denver, CO, 2012

Lei B., Xu G., Feng M., van der Heijden F., Zou Y., de Ridder D., Tax D.M. Classification, parameter estimation and state estimation: an engineering approach using MATLAB. John Wiley & Sons; 2017 May 30.

Leite V.C., da Silva J.G., Veloso G.F., da Silva L.E., Lambert-Torres G., Bonaldi E.L., de Oliveira L.E. Detection of localized bearing faults in induction machines by spectral kurtosis and envelope analysis of stator current. IEEE Transactions on Industrial Electronics. 2015 Mar;62(3):1855-65.

Meyer L., Ahlgren F., Weichbrodt B. (1980) “An analytic model for ball bearing vibrations to predict vibration response to distributed defects,” Journal of Mechanical Design, vol. 102, April 1980, pp. 205–210

Onel I., Dalci K., Senol I. (2005) “Detection of outer raceway bearing defects in small induction motors using stator current analysis” Sadhana Vol. 30, Part 6, December 2005, pp. 713–722

Orchard M. and Vachtsevanos G., “A Particle Filtering-Based Framework for Real-Time Fault Diagnosis and Failure Prognosis in a Turbine Engine,” Mediterranean

Conference on Control and Automation MED'07, Athens, Greece, July 2007.

Orchard M., Hevia-Koch P., Zhang B., Tang L. (2013) Risk Measures for Particle-filtering-based State-of-charge Prognosis in Lithium-ion Batteries, IEEE Trans. Ind. Electron, 60(11), pp. 5260-5269

Paris P., Erdogan F. (1963), A critical analysis of crack propagation laws, Journal of Basic Engineering, Transactions of the American Society of Mechanical Engineers, December 1963, pp.528-534.

Singleton RK, Strangas EG, Aviyente S. Extended Kalman filtering for remaining-useful-life estimation of bearings. IEEE Transactions on Industrial Electronics. 2015 Mar;62(3):1781-90.

Yu J., Ziehl P., Matta F., Pollock A. (2013) Acoustic emission detection of fatigue cracks in welded cruciform joints, Journal of Constructional Steel Research, 86, pp. 85-91.

Zhang B., Georgoulas G., Orchard M., Saxena A., Brown D., Vachtsevanos G., Liang S., Rolling Element Bearing Feature Extraction and Anomaly Detection Based on Vibration Monitoring, 2008 Mediterranean Conference on Control and Automation, June 2008, Ajaccio, France, pp1792-1797

Zhang B., Sconyers C., Byington C., Vachtsevanos G. (2011) A probabilistic fault detection approach: application to bearing fault detection, IEEE Trans. Ind. Electron, 58(5), pp. 2011-2018.

Zhang B., Sconyers C., Orchard M., Patrick R., Vachtsevanos G. Fault Progression Modeling: An Application to Bearing Diagnosis and Prognosis, 2010 ACC

Zhao G., Zhang G., Zhang B. Niu G., Hu C., Bearing Health Condition Prediction Using Deep Belief Network, Annual Conference of Prognostics and Health Management Society, 2017, Orlando FL

Zhou H, Chen J, Dong G, Wang R. Detection and diagnosis of bearing faults using shift-invariant dictionary learning and hidden Markov model. Mechanical systems and signal processing. 2016 May 1;72:65-79.

BIOGRAPHIES

Edward W. Mayfield received the B.S.E degree in 2016 and is currently pursuing the M.S. degree in electrical engineering at the University of South Carolina. His research focus is in health management systems for rotating machinery and he is also currently working in new product development at Samtec South Carolina Design Center.

Guangxing Niu received the B.A. degree from North University of China, Taiyuan, China, in 2014, and the M.S.E. degree from Harbin Institute of Technology, Harbin, China, in 2016, both in electrical engineering. He is currently working toward the Ph.D. degree in electrical engineering from the University of South Carolina, Columbia, SC, USA. His current research focuses on the data-driven-based algorithms of diagnosis and prognosis for lithium ion batteries and industrial systems.

Bin Zhang received the B.E. and M.E. degrees from the Nanjing University of Science and Technology, Nanjing, China, respectively, and the Ph.D. degree from Nanyang Technological University, Singapore, in 2007. He was with Research and Development, General Motors, Detroit, MI, USA, Impact Technologies, Rochester, NY, USA, and the Georgia Institute of Technology, Atlanta, GA, USA. He is currently with the Department of Electrical Engineering, University of South Carolina, Columbia, SC, USA.

Paul Ziehl received his BS in Architectural Engineering from Cal Poly San Luis Obispo and his MS and PhD from UT Austin in Civil Engineering, Structures. His research interests include structural monitoring and prognosis. He currently serves as Assistant Dean for Research and Professor of Civil and Environmental Engineering at University of South Carolina.